Plasma Polymerized Organosilicon Thin Films for Volatile Organic Compound (VOC) Detection

Ghadi Dakroub [1,2], **Thomas Duguet** [1], **Corinne Lacaze-Dufaure** [1], **Stéphanie Roualdes** [2], **Arie van der Lee** [2], **Diane Rebiscoul** [3] and **Vincent Rouessac** [2,*]

1   CIRIMAT, University of Toulouse, CNRS UMR 5085, INP-ENSIACET, 31062 Toulouse, France
2   IEM, CNRS UMR 5635, Univ Montpellier, CEDEX 5, 34095 Montpellier, France
3   ICSM, CEA, CNRS UMR 5257, Univ Montpellier, 30216 Bagnols-sur-Cèze, France
*   Correspondence: vincent.rouessac@umontpellier.fr

Abstract: Plasma polymerized (PP) thin films deposited in a soft or intermediate plasma discharge from hexamethyldisiloxane (HMDSO) were developed as sensors for the detection of volatile organic compound (VOC) vapors. Energy dispersive X-ray spectroscopy (EDX) and X-ray reflectometry (XRR) were performed to determine the organosilicon films' elemental composition and density. Spectroscopic ellipsometry measurements were carried out to determine the refractive index of the films. Quartz crystal microbalance (QCM) and ellipsometry coupled to vapor sorption were used to investigate the sorption mechanism of several VOC vapors into the films as a function of the plasma deposition conditions. The density and the refractive index of the PP-HMDSO films increased with the plasma energy due to a different chemical composition and different proportion of free volumes in the material network. The PP-HMDSO films showed different affinities towards the VOC vapors depending on the plasma discharge energy. The films elaborated in the lowest plasma energy revealed a good sensitivity towards the VOCs, especially toluene (one of the BTEX vapors), compared to the other films deposited under higher plasma energy. In addition, the selectivity between toluene and other non-BTEX VOCs such as heptane and ethanol decreased to become zero while increasing the plasma energy.

Keywords: organosilicon; VOCs; sorption; thin films; QCM; ellipsometry

1. Introduction

Volatile organic compounds (VOCs) are toxic gases present in ambient air because of natural resources and human activities, such as the transportation sector or industrial processes.

Several materials have been synthetized for VOC detection, such as activated carbons [1], zeolites [2] and metal oxide materials [3]. Activated carbons are useful materials for VOC detection due to their microporous structure, large surface area and fast adsorption capability [1,4]. However, these materials reveal experimental problems such as their high flammability [5] and difficulty of regeneration [6] that restrain their use in such applications. Alternatively, zeolite materials seem to be useful candidates for VOC detection thanks to their high specific area, non-toxic behavior and high thermal stability [7,8]. Nevertheless, zeolites are hydrophilic and thus need a surface treatment to turn hydrophobic [9]. Furthermore, the detection of VOCs using zeolite materials requires a compact gas chromatograph (GC) system to analyze the gaseous effluent desorbed from the zeolite by thermal heating [10]. Numerous other studies have focused on the sorption of toluene and benzene on metal oxide materials such as ZnO and WO_3 [11,12]. A good sensitivity has been obtained towards benzene and toluene detection with a fast response. Nevertheless, these materials have shown poor selectivity against other VOCs such as acetone and ethanol, except at high operating temperatures [13,14]. On the other hand, metal oxide materials

show an important sensitivity to water vapor that highly reduces their sensitivity towards VOCs [15].

Finally, organic polymers represent a very competitive class of materials for VOC detection, for instance polyisobutylene (PIB) and polybutadiene (PBD) or organosilicon (SiOCH) polymers like polydimethylsiloxane (PDMS) and poly (methylphenylsiloxane) [16–18]. Organosilicon polymers present a high affinity to VOCs and especially to benzene, toluene, ethylbenzene and xylene, denoted as BTEX. These polymers are widely used in chromatographic columns for VOC detection. They have received remarkable attention for VOC sensing applications due to their swelling effect upon VOC absorption [19,20]. In addition, they are non-toxic [21] and thermally and chemically stable [22] with high surface hydrophobicity, which is important for the detection of non-polar molecules such as BTEX [23]. More particularly, organosilicon materials prepared by Plasma-Enhanced Chemical Vapor Deposition (PECVD) are currently used in NEMS (Nano Electromechanical Devices) devices for organic vapor detection not only because of their high affinity towards the target molecules, but also because they equilibrate more rapidly and reversibly with the sorbed species than bulk polymers due to their micrometric thickness [24]. Sabahy et al. [25] have studied PECVD-deposited SiOCH thin films for BTEX sensing applications. By varying the precursors and plasma deposition conditions, i.e., plasma power, monomer flux and O_2 flow rate, different SiOCH chemical compositions have been synthesized and the effects of the chemical bonds on toluene sorption (as BTEX representative) have been investigated. The authors have shown that SiOSi bonds play the major role in toluene adsorption due to the free volumes created by these bonds in the films, either issued from the SiOSi chains flexibility or directly related to the high methyl bonds proportion. In addition, they have concluded that Si-OH bonds are detrimental to toluene sorption. This result can be related to water vapor adsorption on the film's surface after deposition favored by the polarity of the Si-OH bonds, preventing toluene adsorption. The impact of Si-(CH$_3$) bonds has also been studied. A high concentration of Si-CH$_3$ bonds is detrimental to toluene adsorption; however, a compromise between low Si-CH$_3$ concentration and films' hydrophobicity is necessary. An optimized composition of the plasma-SiOCH thin film could be obtained with a higher affinity towards BTEX than conventional polymers. Finally, Boutamine et al. [26] have elaborated plasma polymerized thin films from HMDSO and investigated VOC sorption using a quartz crystal microbalance (QCM). The affinity toward VOCs such as ethanol, methanol and chloroform has been correlated to the material surface hydrophobicity, the molecules' size and to the free volumes within the films' network.

In the present work, we aim at elaborating performant materials for VOC detection that can be used in the manufacturing of portable gravimetric sensors that are competitive in term of compactness when compared to gas chromatograph systems (GC). As previously mentioned, due to their well-known low thickness, hydrophobicity, non-toxicity, thermal stability and high affinity to VOCs, plasma polymerized organosilicon thin films appear as perfect candidates for the targeted application.

In a recent paper [27], we thoroughly investigated morphological and structural characterizations of plasma polymerized (PP-) organosilicon materials prepared in a microwave plasma discharge from HMDSO. By the way, this easy-to-use precursor has been largely investigated for years [28] to produce organosilicon PP-HMDSO films at deferent plasma conditions for a variety of applications. The characterization of the bulk chemical composition studied by FTIR spectroscopy and quantitative ^{29}Si solid state NMR revealed a high amount of SiOC$_3$ termination in the films deposited under soft plasma conditions (low plasma energy) due to the low monomer fragmentation. Moreover, linear SiO$_2$C$_2$ chains that are close to PDMS chains were present in the material bulk deposited under soft plasma conditions. However, under hard plasma conditions (high plasma energy), the high monomer fragmentation reduced the amount of SiOC$_3$ terminations and favored the introduction of carbon/hydrogen atoms into the material bulk, leading to the formation of new chemical bonds such as Si-O-C, Si-CH$_2$-Si and Si-H. Furthermore, the amount of the linear SiO$_2$C$_2$ chains decreased in the material bulk at hard plasma conditions. These

major evolutions introduced chemical and structural disorder in the bulk of the elaborated films. The surface chemical composition detected using a combination between X-ray photoelectron spectroscopy (XPS) and density functional theory (DFT) calculations also showed a chemical modification while increasing the plasma energy. In fact, the number of $SiOC_3$ units increased and the amount of SiO_2C_2 units decreased. In addition, the formation of new chemical bonds on the surface, such as Si-CH$_2$-Si, Si-H, Si-O-C and Si-OH, has been confirmed, leading to some disorder in the chains' formation. Furthermore, the hydrophobicity of the films was investigated; the PP-HMDSO films showed a hydrophobic character, especially at low plasma energy (close to 103°). As a conclusion of this previous paper, the films deposited under soft plasma conditions showed quite a similarity to conventional PDMS. On the contrary, the films elaborated under hard plasma conditions lost their PDMS-like character and changed to more hybrid structures due to the new bond formation and enhancement of the structural disorder in the films.

In the present study, some selected films among the previously prepared SiOCH plasma polymerized thin films are more deeply characterized by energy dispersive X-ray spectroscopy (EDX) for the elemental composition, X-ray reflectometry (XRR) for the density and ellipsometry for the film thickness and refractive index. We have decided to select films synthesized in a finer W/F range (5 W/sccm to 20 W/sccm) for which the influence of the chemical composition modification on sorption properties is more pronounced. The deposition conditions of the three samples WF5, WF10 and WF20 are reproduced from [27] and presented in Table 1. The thicknesses of the samples are different from those presented in the previous work due to a different deposition duration. In order to study the affinity of the synthetized films towards VOCs, the surface acoustic wave (SAW) technique can be used [29]. In this study, quartz crystal microbalance (QCM) and ellipsometry, both coupled with gas sorption techniques, were used. Finally, the impact of the chemical composition on the affinity towards VOCs is analyzed, leading to the identification of an optimized SiOCH film for VOC gravimetric sensing applications.

Table 1. MW-PECVD thin film deposition parameters issued from [27].

Sample	Plasma Power (W)	HMDSO Flux (sccm)	W/F	Deposition Pressure ($\times 10^{-3}$ mBar)	Average Thickness (nm)	Average Growth Rate (nm/min)
WF5	20	4	5	10.5	332	108
WF10	20	2	10	7.5	344	63
WF20	20	1	20	5.9	296	30

2. Materials and Methods

2.1. Thin Films Synthesis

As described previously in detail [27], HMDSO plasma polymerized thin films were elaborated in a microwave MW-PECVD reactor supplied by Boreal Plasmas (Andrezieux-Boutheon, France). The deposition reactor is a stainless steel cylindrical chamber with a limit pressure of 10^{-7} mbar. The microwave antennas supply the plasma power in the chamber from a MW power supply at a frequency of 2.45 Hz (Sairem, Décines-Charpieu, France). The applicators are distributed on the top of the chamber, forming a rectangular lattice matrix (3 × 2). This distribution ensures the homogeneity of the discharge and the deposited films. Vapor of HMDSO precursor (Sigma-Aldrich, Saint-Louis, MO, USA ≥98.5%) was injected into the chamber using a low-ΔP mass flow controller (Brooks Instrument, Hatfield, USA). All depositions were performed at room temperature, while the plasma input power was fixed at 20 W and the monomer flux F was varied from 1 sccm to 4 sccm (Table 1).

2.2. Characterizations

EDX (Silicon Drift Detector (SDD), X-MaxN, Oxford Instruments, Abingdon-on-Thames, UK) analyses were performed in order to obtain the elemental composition of the

PP-HMDSO films. All the thicknesses of the deposited PP-HMDSO films were compatible with the detection characterization volume of the EDX, i.e., much over ~500 nm in depth from the surface.

X-ray reflectometry (XRR) analyses were carried out using a Bruker (Billerica, MA, USA) D8 diffractometer with Cu-Kα1 (λ = 0.154 nm) radiation. Standard symmetric Bragg–Brentano θ-2θ scans were used for the data collections from 2θ = 0 to 4° (q_{max} = 0.2844 Å^{-1}) with an angular step size of 0.002°, employing small opening and receiving slits and suitable attenuation foils for the measurements in the vicinity of the direct beam. X-ray reflectometry probes the electron density profile of a thin film perpendicular to the surface and therefore symmetric scans are adapted for these measurements as the momentum transfer q is perpendicular to the surface. XRR measurements allowed the determination of the electronic density (ρ_e) from the limit angle of total reflection (critical angle) θ_c, using (1), extracted from Figure 1:

$$\theta_c = \sqrt{\frac{\lambda^2 r_0}{\pi} \rho_e} \tag{1}$$

where λ is the wavenumber and r_0 is the electron radius.
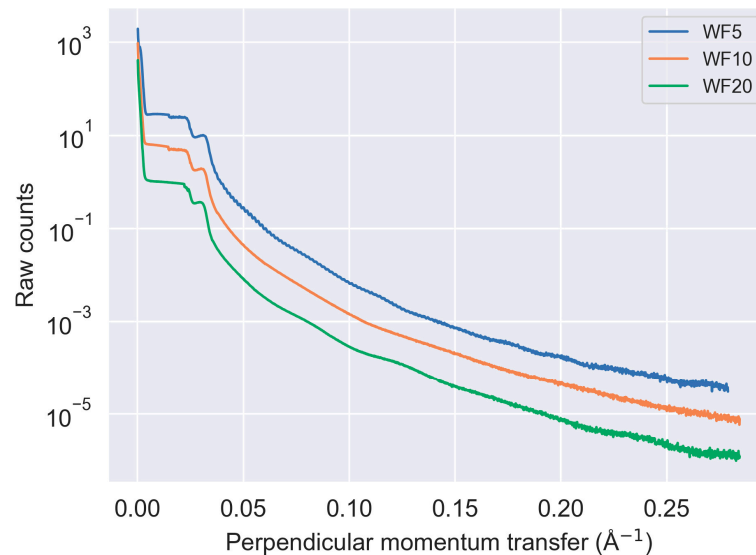
Figure 1. X-ray reflectivity curves of the deposited films. The curves have been slightly displaced vertically for better visibility.

The elemental composition determined by EDX and the electronic density calculated by XRR analyses lead to the mass density (ρ_m) of the PP-HMDSO films using (2):

$$\rho_m = \rho_e \frac{\sum C_j A_j}{N_A \sum C_j Z_j} \tag{2}$$

where C_j is the percentage of an element j in the PP-HMDSO chemical composition given by EDX analysis, Z_j its atomic number, A_j its atomic mass and N_A the Avogadro number.

The error on the density value is estimated to be ±0.03 g/cm^3. This error is due to the zero-point error (sample height and/or goniometer) and the unknown hydrogen content which is needed to convert the electron density to the mass density.

Thin films' refractive indexes and thicknesses were determined by spectroscopic ellipsometry (Semilab GES5E, Budapest, Hungary) at atmospheric pressure. The angle of incidence was fixed at 70° and the collected data range was from E = 1.24 eV to E = 4.25 eV. In the article, the refractive index was given at λ = 633 nm, but the data were fitted in the full light range using a composition of the Cauchy transparent dispersion law and a

Lorentz absorption term towards the UV range. The fit quality exceeds 0.99 in the full range for all analyses.

In situ ellipsometry coupled to sorption measurements [30] was carried out by exposing PP-HMDSO thin films to toluene or ethanol at controlled vapor pressures. Samples were placed in a lab-made optical cell equipped with pressure and temperature control systems. The cell was initially pumped down to 0.05 mbar before any sorbate introduction. Afterwards, toluene or ethanol gas vapors were introduced inside the cell gradually up to its saturation pressure to obtain the refractive index isotherm. Please note that this simple lab-made setup cannot give information about the depth profile from the surface of the concentration of sorbed molecules, unlike neutron reflectometry [31,32], which can do so.

QCM (Inficon, Bad Ragaz, Switzerland) measurements for gas sorption and desorption were performed using an Inficon STM2 thin film oscillator monitor driven by lab-made data collection software in order to obtain mass uptake sorption isotherms. PP-HMDSO thin films were deposited on an AT-cut gold-covered quartz (6 MHz). The coated quartz was placed in a chamber under vacuum in which gas vapors were introduced systematically up to its saturated vapor pressure value at room temperature. For all the measurements, the quartz was thermally stabilized at 25 °C using water circulation and a bath. The frequency variation (Δf) is proportionally linked to the mass variation (Δm) due to gas vapor sorption or desorption according to Sauerbrey's equation [33] (3):

$$\Delta f = \frac{-f_q^2 \times \Delta m}{C \times \rho_q \times S} \tag{3}$$

where f_q = 6 MHz is the frequency of the uncoated quartz, depending on the quartz size. $S = 0.5$ cm^2 represents the surface area of the deposited film, $\rho_q = 2.65$ g/cm^3 is the density of the quartz and $C = 1.67 \times 10^5$ cm/s is an apparatus constant.

The mass of the deposited film can be neglected compared to the mass of the quartz. Thus, the density of the coated quartz is equal to the density of the pristine quartz (ρ_q). Since the masses of both the quartz and the films are constant, Δm corresponds to the sorbed vapor mass uptake (m_{sorbed}) by the thin films. Therefore, m_{sorbed} of the deposited thin films was determined using (4):

$$m_{sorbed}\left(P/P_0\right) = \frac{-\Delta f}{f_q^2}\, 1.67 \times 10^5 \times \rho_q \times S \tag{4}$$

The collected data were converted into mass uptake and isotherms of m_{sorbed} as a function of relative pressure (P/P_0) were plotted, P_0 being the saturated pressure of the used vapors (Table 2). For isotherms under air, the maximal collected absolute pressure is 1 bar.

Table 2. Saturated pressure (P_0) of the vapors used in this work.

Vapor	P_0 at 25 °C (mbar)
Water	31.7
Ethanol	75.9
Heptane	60.7
Toluene	37.1

3. Results

In this section, the elemental composition and physical properties such as the density and refractive index of the PP-HMDSO thin films as well as their response towards several VOC vapors separately are presented.

The elemental composition determined by EDX reveals a quite similar composition of the three films. The carbon, oxygen and silicon percentages are at% 52.2 ± 0.8, 22.4 ± 0.8

and 25.4 ± 0.8, respectively, revealing a composition close to that of conventional PDMS, i.e., C:50at%, O:25at% and Si:25at%.

The calculated density and the refractive index of the PP-HMDSO thin films are presented in Figure 2. The film deposited at 5 W/sccm reveals a low density (1.35 g/cm³) compared to the films deposited at 10 W/sccm and 20 W/sccm (values close to 1.45 g/cm³). In addition, the refractive index of the SiOCH films increases from 1.52 for the films deposited at 5 W/sccm to values close to 1.57 for the films deposited at 10 W/sccm and 20 W/sccm. In fact, the variation of the films' density generates a variation of the deposited films' refractive index while increasing the W/F parameter. Indeed, the well-known Clausius–Mossotti Equation (5) reveals the influence of the material density on the dielectric constant or the refractive index (n), since $n = \varepsilon^2$ in the visible optical range:

$$\frac{\varepsilon - 1}{\varepsilon + 2} = \frac{\rho_m}{3\varepsilon_0} \sum_{i=1}^{k} N_i \alpha_i \tag{5}$$

where ρ_m is the density of the elaborated SiOCH films, ε_0 is the vacuum permittivity, ε is the dielectric constant, $k = 3$ corresponding to the three atoms C, O, Si, N_i is the number of atoms i per cm³ and α_i is the polarizability of atom i. Figure 2 confirms the relation between the refractive index and the mass density, which is determined from XRR optical measurements, i.e., electron density adjusted with elemental composition.
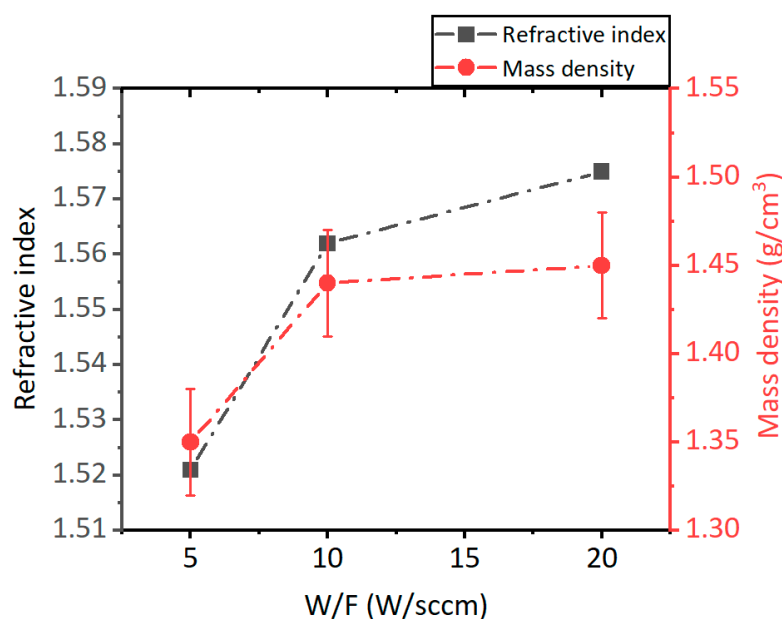
Figure 2. The refractive index and the calculated density of the deposited films.

In such low-pressure MW-PECVD plasma, a higher W/F ratio leads to more inorganic (less organic) deposited SiOxCyHz material that is more crosslinked and less flexible with smaller interchain spaces. Thus, plasma operating conditions may influence the ability of sorption that depends on the chemistry but also on the network rigidity and free volume. For that, the responses of the PP-HMDSO thin films towards hydrocarbon and ethanol vapor sorption studied using QCM are presented in Figure 3. In this study, heptane and ethanol vapors were used as representatives for VOCs and toluene vapor as representative for BTEX gases. Ethanol vapor was used as a reference in order to compare its sorption to hydrocarbons. The calculated mass uptake value represents the mass of the vapor sorbed by the thin film. Moreover, as the mass uptake increases proportionally with the film thickness, it can be concluded that the molecules are not only adsorbed on the film surface but are also absorbed in the bulk. Therefore, the mass uptake was simply divided by the film thickness value to obtain the concentration of absorbed molecules per material volume

unity even if no conclusion can be written on how the absorbed molecules are diluted in the material matrix, homogeneously or in a gradient concentration from the surface to the bulk. The uncertainty on the mass uptake value is taken as the standard deviation over three repeated QCM measurements.
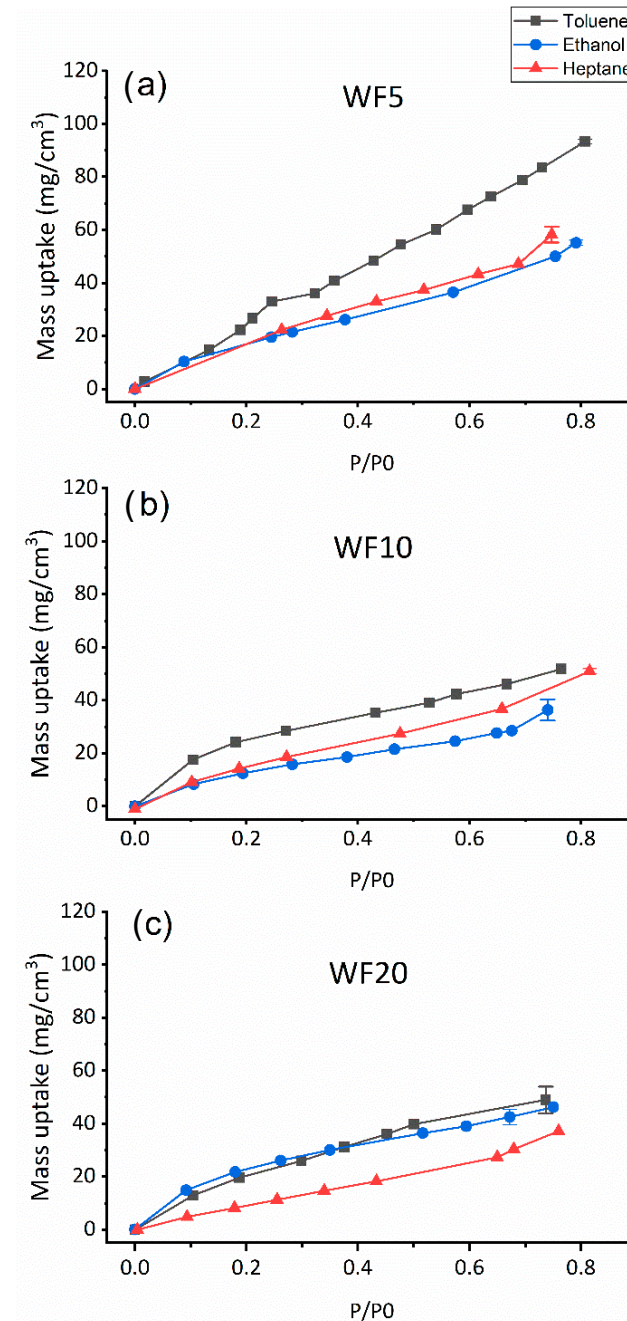
Figure 3. QCM sorption isotherms (25 °C) showing the evolution of ethanol, heptane and toluene vapor mass uptake with P/P0 (P0 being the saturated vapor pressure) for (**a**) WF5, (**b**) WF10 and (**c**) WF20.

As observed in Figure 3, the mass uptake of the gas vapors increases with increasing the relative pressure P/P0 for all the PP-HMDSO thin films, P0 being the saturated vapor pressure at the temperature of the quartz, stabilized at 25 °C. The WF5 film shows a linear increase of the toluene uptake mass up to 100 mg/cm^3 at a relative pressure equal to 0.8. Moreover, the heptane and ethanol uptake masses also reveal a linear increase but to lower values (close to 60 mg/cm^3) compared to toluene. Thus, the WF5 deposit shows a better

affinity to toluene vapor than the two other vapors. The WF10 deposit shown in Figure 3b illustrates weaker responses to the three vapors compared to the WF5 deposit, especially to toluene vapor. Furthermore, the toluene isotherm of the WF10 film shows a non-linear increase. However, the final mass uptake for toluene vapor is higher than the two other vapor masses, especially compared to the ethanol uptake mass, indicating a better affinity for WF10 towards toluene vapor. Moreover, WF5 and WF10 deposits reveal a slightly better affinity towards heptane vapor compared to ethanol vapor. On the other hand, the deposit with the higher W/F (WF20) shows similar isotherms for toluene and ethanol. The toluene and ethanol isotherms show a non-linear uptake mass increase showing a fast sorption between 0 and 0.2 P/P0 followed by a slower sorption between 0.2 and 0.8 P/P0. Furthermore, the heptane vapor isotherm reveals mass uptakes lower than those of toluene and ethanol, suggesting a weaker affinity towards heptane vapor compared to toluene and ethanol vapors.

Figure 4 focuses on the comparison between the toluene sorption isotherms of the three PP-HMDSO thin films. A remarkable change in the sorption isotherms is shown while increasing W/F from 5 W/sccm to 10 W/sccm. However, identical isotherms are observed for the films elaborated at 10 W/sccm and 20 W/sccm.
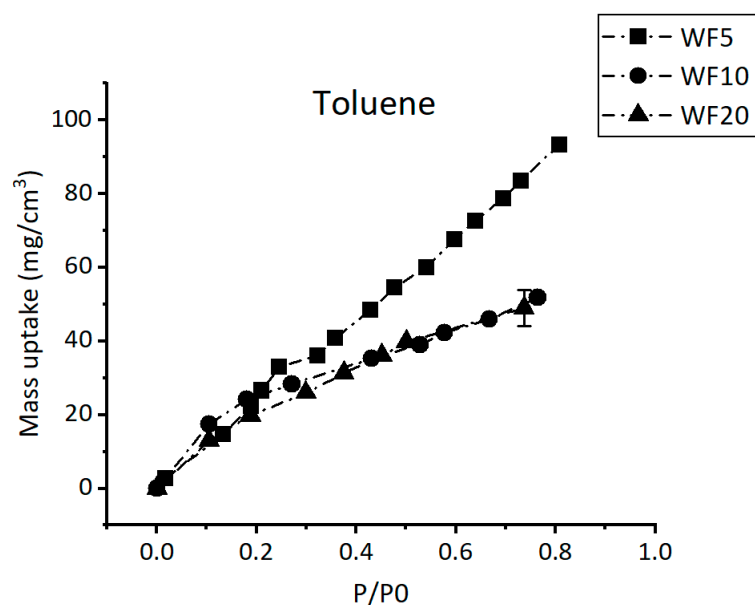
Figure 4. QCM toluene sorption isotherm (25 °C) of films synthesized at different W/F values showing the evolution of the mass uptake vs. P/P0, P0 being the saturated vapor pressure at 25 °C.

In fact, the toluene isotherm loses its linearity while increasing W/F from 5 W/sccm to 10 W/sccm and the final uptake mass value decreases from 100 mg/cm^3 to approximately 50 mg/cm^3. These variations indicate a slower sorption process, especially at lower P/P0 values, typically between 0 and ~0.2, and a weaker affinity for WF10 and WF20 deposits towards toluene compared to WF5.

The responses of the PP-HMDSO thin films towards toluene and ethanol vapors was also studied using ellipsometry coupled to vapor sorption. Figure 5 shows the swelling of the PP-HMDSO thin films along the normal to the film when exposed to toluene or ethanol vapors. We assume in this study that the swelling is homogenous despite the mechanical constraints present between the film and the silicon support. This model indicates that the COV concentration should vary along the depth of the film from the surface. d0 is the thickness measured under vacuum and d is the thickness measured as a function of the stabilized environment pressure, i.e., after enough time to attend to the equilibrium between the gaseous molecules pressure and the absorbed molecules pressure inside the material bulk.
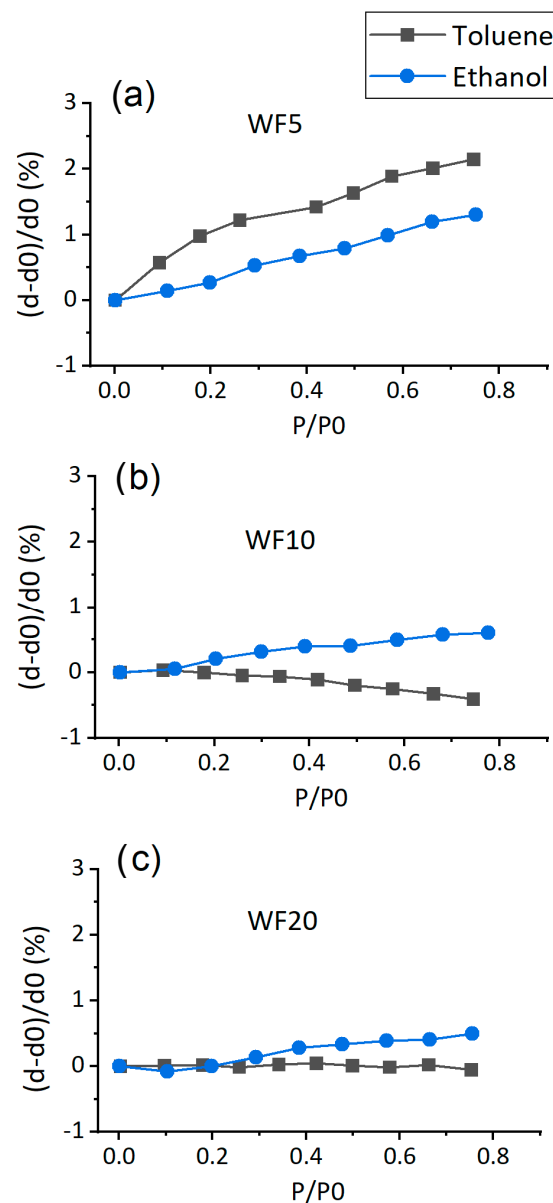
Figure 5. Swelling of the elaborated PP-HMDSO thin films while exposed to toluene or ethanol atmospheres, P0 being the saturated vapor pressure. d0 is the initial film thickness under vacuum and d is its thickness under P/P0 of toluene of ethanol. (**a**) WF5, (**b**) WF10 and (**c**) WF20.

The swelling phenomenon of the SiOCH films when exposed to VOCs is due to the penetration of the gas vapors into the material bulk through the free volumes present in the polymer network. Figure 5 reveals that the thickness of WF5 thin film improves while increasing toluene or ethanol vapor relative pressure. However, WF5 reveals a higher swelling rate for toluene compared to ethanol. Therefore, WF5 shows a better absorption of toluene molecules compared to ethanol molecules. On the other hand, WF10 and WF20 isotherms indicate a low film-swelling rate while exposed to both vapors. Nevertheless, the WF10 swelling rate is slightly better when exposed to ethanol compared to the swelling rate in the presence of toluene, for which a slight film contraction is observed.

Since the WF5 deposit revealed the better affinity towards toluene, it might be interesting to study the affinity of the WF5 deposit towards humidity. Figure 6 shows a comparison between the WF5 deposit responses towards toluene and water vapor. The water vapor isotherm reveals extremely low mass uptakes compared to the toluene, indicating a very weak sensitivity of WF5 towards water vapor.
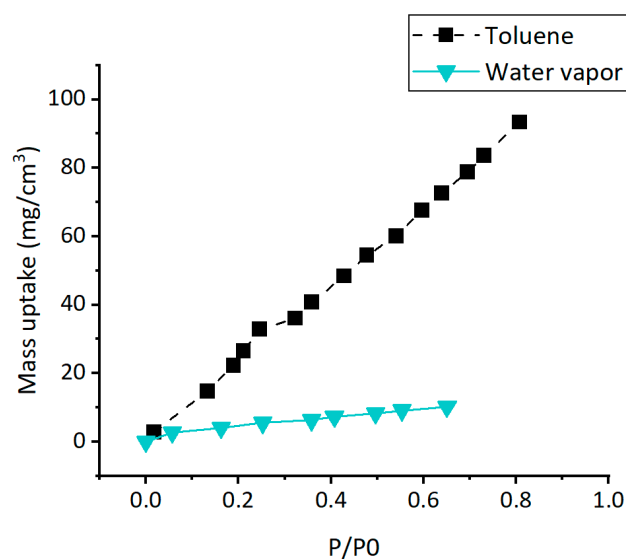
Figure 6. Comparison of the adsorption of water vapor and toluene on the WF5 deposit as a function of the relative pressure (P0 being the saturated vapor pressure at measurement temperature, 25 °C).

4. Discussion

4.1. Density and Refractive Index

The density change shown in Figure 1 while increasing W/F from 5 W/sccm to 10 W/sccm and 20 W/sccm is probably the result of the introduction of carbon atoms into the film skeleton to replace the oxygen atom in the Si-O-Si chains, creating new bonds such as Si-O-C and $Si-CH_2-Si$. In fact, the Si-O-Si chains that form the material skeleton of organosilicon films are responsible for creating free volumes in the material network and decreasing the density [34]. However, the replacement of these bonds by Si-O-C and $Si-CH_2-Si$ bonds and the disorder introduced in the films' network at higher W/F values shown in our previous work [27] reduce the proportion of free volumes in the material bulk, causing the increase of the films' density. Furthermore, the refractive index enhancement with W/F can be demonstrated by the films' density increase (Equation (1)) due to the reduction of the free volume proportion. In addition, the refractive index improvement can be a result of another factor, which is the electronic polarizability increase due to the incorporation of carbon atoms into the material bulk. In fact, the incorporation of carbon atoms can generate variations on chemical bond angles in the SiOCH films, leading to the reduction of the number of dipole moments in the system and hence increasing the polarizability [35–37]. Accordingly, the remarkable differences in the densities and refractive indexes between WF5 on the one hand and WF10/WF20 on the other hand confirms the division of the soft plasma range into two groups. In fact, the weak variation in the energetic plasma character between WF5 and WF10 enhances the PP-HMDSO films' density and refractive index by changing the film composition and reducing the proportion of free volumes in the SiOCH film.

4.2. Gas Sorption Performance

The SiOCH films' performance towards VOC vapor sorption depends strongly on the chemical composition and the structure of the films. In the WF5 material, the sorption selectivity between toluene and ethanol is due to the hydrophobicity difference of the films' surface shown previously [27] that gives a higher affinity towards the non-polar toluene. In addition, the better response for toluene compared to heptane can be attributed to the molecule size and chain length for linear hydrocarbons. We assume that the absorption of toluene into the films is greater than the absorption of heptane, which mainly remains adsorbed on the surface. In fact, Zheng Yang et al. concluded that alkanes lie flat on silica surfaces and the molecules' adsorption on the surface increases with chain length [38]. We

have also studied butane vapor sorption on the WF5 sample. Butane vapor showed good affinity towards WF5. The butane sorbed mass was 36 mg/cm^3 at P/P0 = 0.34 greater than the heptane sorbed mass (27 mg/cm^3) at the same P/P0 value. Thus, WF5 thin film revealed a better affinity towards butane vapor than heptane because of its shorter chain length. This result is consistent with the work of Zheng Yang et al. [38].

The decrease in the toluene uptake mass and the loss of linearity of the isotherm, i.e., the slower sorption process while increasing W/F to 10 W/sccm and 20 W/sccm, suggest a toluene sensitivity decrease for the materials elaborated at higher plasma energy. In fact, the reduction of the free volume's proportion detected in the density section weakens the toluene sorption process. In addition, the formation of Si-OH bonds on the surface at higher W/F favors a rapid water adsorption on the surface and can be detrimental for toluene adsorption [25]. These chemical and physical modifications can also explain the loss of the selectivity between toluene and ethanol vapors shown especially in the WF20 deposit. Furthermore, the weak hydrophobicity of WF20 compared to the two other samples and the large size of the heptane molecule result in lower sorbed masses compared to ethanol and toluene. As mentioned before, alkanes lie flat on the silica surface [38]; this conclusion can explain the low penetrated masses of heptane compared to toluene in all the PP-HMDSO thin films.

Similarly, the ellipsometry coupled to the sorption results reveals a loss of the swelling rate during toluene sorption for WF10 and WF20, indicating a weak affinity towards toluene vapor. In fact, the material density increases and the chemical composition modifications observed in WF10 and WF20 prevent the film swelling, leading to a decrease in the gas vapors' penetration into the material. In addition, the swelling phenomenon can be linked to the crosslinking degree of the films and the bonds' chemical composition. In fact, a low crosslinking rate induces the swelling of the polymeric chains [20]. Furthermore, the flexibility of the Si-O-Si chains facilitates the penetration ability of VOCs, unlike Si-O-C chains that are less flexible. Hence, the low films' swelling rate can suggest an improvement in the WF10 and WF20 hardness provoked by the structural and chemical deformation of the films' network shown in Dakroub et al. [20,27,33]. On the other hand, we assume that the decrease in the WF10 film thickness while exposed to toluene vapor is due to the absence of the free volume that prevents toluene vapor absorption and the lower rigidity of the WF10 film compared to WF20. Finally, the ellipsometry coupled to the sorption results is in accordance with QCM results showing a better affinity for WF5 towards toluene vapor compared to ethanol vapor.

Finally, the bigger size of the sorbed molecule of toluene seems to be the main reason that the swelling of the film is more important compared to that of heptane, which is a smaller and linear molecule. But chemistry is also important: heptane and ethanol ad/absorption are different because of the hydrophobicity of the surface, which depends on the plasma conditions: the surface of WF5 is different from that of WF10 and that of WF20.

Furthermore, the WF5 affinity towards water vapor was studied in order to determine the effect of humidity on toluene sorption. WF5 revealed a very weak affinity towards water vapors, allowing its performance in humid environments. Indeed, the hydrophobic character of the organosilicon thin films is detrimental to the sorption of water vapor [13]. The mass uptake depends on the concentration of the absorbate spread among the PP-HMDSO network. But the absorbate comes from the surface, i.e., there is absorption if there is adsorption first. The surface of the PP-HMDSO is hydrophobic. Thus, the water concentration inside PP-HMDSO is weak, even if the water molecule is very small.

5. Conclusions

In a previous work, we determined the effect of the plasma energy on the chemical composition and structure of the PP-HMDSO thin films. In the present article, physical properties such as the refractive index and density of the films were presented. In addition,

the effects of the materials' chemical composition and the physical properties on the sorption of VOC vapors were also investigated.

In conclusion, the plasma energy governs the density of the films. In fact, the films' free volume proportion decreases while increasing the plasma energy, leading to a denser material due to the formation of new bonds such as Si-CH$_2$-Si and Si-O-C in the film structure. The chemical composition modification shown previously and the density variation with the plasma energy affect both the sensitivity and the sorption selectivity of the materials towards the VOCs. In fact, the PP-HMDSO thin films elaborated in this study showed different responses towards tested VOC vapors (ethanol, heptane, toluene) despite the small plasma conditions' variation between WF5, WF10 and W20 (5 W/sccm to 20 W/sccm). The WF5 showed good sensitivity towards toluene and good sorption selectivity between toluene and the other tested VOCs compared to the WF10 and WF20 deposits. This is due to the low density and high hydrophobicity ($\approx$103° detected previously in [27]) of the WF5 material as well as a high SiOSi bond amount in the PP-HMDSO network.

Finally, chemical and physical properties play important roles in the vapors' sorption into the organosilicon films. A combination of surface hydrophobicity and free volume size (density) should be optimized in order to achieve a good sensitivity/selectivity to toluene (BTEX) vapor compared to other VOCs.

Author Contributions: Methodology, G.D., T.D., C.L.-D., S.R. and V.R.; software, D.R.; formal analysis, C.L.-D., A.v.d.L. and D.R.; investigation, G.D.; data curation, G.D. and T.D.; writing—G.D., A.v.d.L. and V.R.; review, C.L.-D., S.R. and V.R.; editing, V.R.; supervision, V.R.; funding acquisition, T.D. and V.R. All authors have read and agreed to the published version of the manuscript.

Funding: This research was partially funded by the French Carnot Institute Chimie Balard Cirimat (Ph.D. grant #IEM/PETAB/2018-030).

Institutional Review Board Statement: The study was conducted in accordance with the Declaration of Helsinki, and approved by the Institutional Review Board (or Ethics Committee) of CIRIMAT IEM and ICSM for studies involving humans.

Informed Consent Statement: Informed consent was obtained from all subjects involved in the study.

Data Availability Statement: All research data presented in this article are kept and available at CIRIMAT, IEM and ICSM.

Acknowledgments: We warmly thank the Bertrand Rebière from ICGM-IEM for the EDX analyses.

Conflicts of Interest: The authors declare no conflict of interest.

References

1. Son, H.K.; Sivakumar, S.; Rood, M.J.; Kim, B.J. Electrothermal adsorption and desorption of volatile organic compounds on activated carbon fiber cloth. *J. Hazard. Mater.* **2016**, *301*, 27–34. [CrossRef]
2. Megias-Sayago, C.; Lara-Ibeas, I.; Wang, Q.; Le Calve, S.; Louis, B. Volatile organic compounds (VOCs) removal capacity of ZSM-5 zeolite adsorbents for near real-time BTEX detection. *J. Environ. Chem. Eng.* **2020**, *8*, 103724. [CrossRef]
3. Mirzaei, A.; Leonardi, S.G.; Neri, G. Detection of hazardous volatile organic compounds (VOCs) by metal oxide nanostructures-based gas sensors: A review. *Ceram. Int.* **2016**, *42*, 15119–15141. [CrossRef]
4. Choma, J.; Marszewski, M.; Osuchowski, L.; Jagiello, J.; Dziura, A.; Jaroniec, M. Adsorption properties of activated carbons prepared from waste CDs and DVDs. *ACS Sustain. Chem. Eng.* **2015**, *3*, 733–742. [CrossRef]
5. Zhang, L.; Peng, Y.; Zhang, J.; Chen, L.; Meng, X.; Xiao, F.-S. Adsorptive and catalytic properties in the removal of volatile organic compounds over zeolite-based materials. *Chin. J. Catal.* **2016**, *37*, 800–809. [CrossRef]
6. Dragoi, B.; Rakic, V.; Dumitriu, E.; Auroux, A. Adsorption of organic pollutants over microporous solids investigated by microcalorimetry techniques. *J. Therm. Anal. Calorim.* **2010**, *99*, 733–740. [CrossRef]
7. Kim, K.-J.; Ahn, H.-G. The effect of pore structure of zeolite on the adsorption of VOCs and their desorption properties by microwave heating. *Microporous Mesoporous Mater.* **2012**, *152*, 78–83. [CrossRef]
8. Cosseron, A.-F.; Daou, T.J.; Tzanis, L.; Nouali, H.; Deroche, L.; Coasne, B.; Tchamber, V. Adsorption of volatile organic compounds in pure silica CHA,* BEA, MFI and STT-type zeolites. *Microporous Mesoporous Mater.* **2013**, *173*, 147–154. [CrossRef]
9. Kawai, T.; Tsutsumi, K. Evaluation of hydrophilic-hydrophobic character of zeolites by measurements of their immersional heats in water. *Colloid Polym. Sci.* **1992**, *270*, 711–715. [CrossRef]

10. Lara-Lbeas, I.; Rodríguez-Cuevas, A.; Andrikopoulou, C.; Person, V.; Baldas, L.; Colin, S.; Le Calvé, S. Sub-ppb level detection of BTEX gaseous mixtures with a compact prototype GC equipped with a preconcentration unit. *Micromachines* **2019**, *10*, 187. [CrossRef]
11. Jaaniso, R.; Tan, O.K. *Semiconductor Gas Sensors*; Elsevier: Amsterdam, The Netherlands, 2013; ISBN 9780857098665.
12. Balouria, V.; Kumar, A.; Samanta, S.; Singh, A.; Debnath, A.K.; Mahajan, A.; Bedi, R.K.; Aswal, D.K.; Gupta, S.K. Nano-crystalline Fe$_2$O$_3$ thin films for ppm level detection of H$_2$S. *Sens. Actuators B Chem.* **2013**, *181*, 471–478. [CrossRef]
13. Raut, B.T.; Godse, P.R.; Pawar, S.G.; Chougule, M.A.; Bandgar, D.K.; Patil, V.B. Novel method for fabrication of polyaniline–CdS sensor for H$_2$S gas detection. *Measurement* **2012**, *45*, 94–100. [CrossRef]
14. Zhu, Z.; Kao, C.-T.; Wu, R.-J. A highly sensitive ethanol sensor based on Ag@TiO$_2$ nanoparticles at room temperature. *Appl. Surf. Sci.* **2014**, *320*, 348–355. [CrossRef]
15. Gong, J.; Chen, Q.; Lian, M.-R.; Liu, N.-C.; Stevenson, R.G.; Adami, F. Micromachined nanocrystalline silver doped SnO$_2$ H$_2$S sensor. *Sens. Actuators B Chem.* **2006**, *114*, 32–39. [CrossRef]
16. Grate, J.W.; Kaganove, S.N.; Bhethanabotla, V.R. Comparisons of polymer/gas partition coefficients calculated from responses of thickness shear mode and surface acoustic wave vapor sensors. *Anal. Chem.* **1998**, *70*, 199–203. [CrossRef] [PubMed]
17. Patrash, S.J.; Zellers, E.T. Characterization of polymeric surface acoustic wave sensor coatings and semiempirical models of sensor responses to organic vapors. *Anal. Chem.* **1993**, *65*, 2055–2066. [CrossRef]
18. Hierlemann, A.; Ricco, A.J.; Bodenhöfer, K.; Dominik, A.; Göpel, W. Conferring selectivity to chemical sensors via polymer side-chain selection: Thermodynamics of vapor sorption by a set of polysiloxanes on thickness-shear mode resonators. *Anal. Chem.* **2000**, *72*, 3696–3708. [CrossRef]
19. Park, C.; Han, Y.; Joo, K.-I.; Lee, Y.W.; Kang, S.-W.; Kim, H.-R. Optical detection of volatile organic compounds using selective tensile effects of a polymer-coated fiber Bragg grating. *Opt. Express* **2010**, *18*, 24753–24761. [CrossRef]
20. Ogieglo, W.; van der Werf, H.; Tempelman, K.; Wormeester, H.; Wessling, M.; Nijmeijer, A.; Benes, N.E. n-Hexane induced swelling of thin PDMS films under non-equilibrium nanofiltration permeation conditions, resolved by spectroscopic ellipsometry. *J. Membr. Sci.* **2013**, *437*, 313–323. [CrossRef]
21. Perrin, J.; Leroy, O.; Bordage, M.C. Cross-Sections, Rate Constants and Transport Coefficients in Silane Plasma Chemistry. *Contrib. Plasma Phys.* **1996**, *36*, 3–49. [CrossRef]
22. Zajíčková, L.; Buršíková, V.; Kučerová, Z.; Franclova, J.; Sťahel, P.; Peřina, V.; Mackova, A. Organosilicon thin films deposited by plasma enhanced CVD: Thermal changes of chemical structure and mechanical properties. *J. Phys. Chem. Solids* **2007**, *68*, 1255–1259. [CrossRef]
23. Andreeva, N.; Ishizaki, T.; Baroch, P.; Saito, N. High sensitive detection of volatile organic compounds using superhydrophobic quartz crystal microbalance. *Sens. Actuators B Chem.* **2012**, *164*, 15–21. [CrossRef]
24. Jousseaume, V.; Yeromonahos, C.; El Sabahy, J.; Altemus, B.; Ladner, C.; Benedetto, K.; Ollier, E.; Faguet, J. Filament Assisted Chemical Vapor Deposited organosilicate as chemical layer for nanometric hydrocarbon gas sensors. *Sens. Actuators B Chem.* **2018**, *271*, 271–279. [CrossRef]
25. El Sabahy, J.; Berthier, J.; Ricoul, F.; Jousseaume, V. Toward optimized SiOCH films for BTEX detection: Impact of chemical composition on toluene adsorption. *Sens. Actuators B Chem.* **2018**, *258*, 628–636. [CrossRef]
26. Boutamine, M.; Bellel, A.; Sahli, S.; Segui, Y.; Raynaud, P. Hexamethyldisiloxane thin films as sensitive coating for quartz crystal microbalance based volatile organic compounds sensors. *Thin Solid Films* **2014**, *552*, 196–203. [CrossRef]
27. Dakroub, G.; Duguet, T.; Esvan, J.; Lacaze-Dufaure, C.; Roualdes, S.; Rouessac, V. Comparative study of bulk and surface compositions of plasma polymerized organosilicon thin films. *Surf. Interfaces* **2021**, *25*, 101256. [CrossRef]
28. Avramov, I.; Radeva, E.; Lazarov, Y.; Grakov, T.; Vergov, L. Sensitivity Enhancement in Plasma Polymer Films for Surface Acoustic Wave Based Sensor Applications. *Coatings* **2021**, *11*, 1193. [CrossRef]
29. de Freitas, A.; Maciel, C.; Rodrigues, J.; Ribeiro, R.; Delgado-Silva, A.; Rangel, E. Organosilicon films deposited in low-pressure plasma from hexamethyldisiloxane—A review. *Vacuum* **2021**, *194*, 110556. [CrossRef]
30. Haacké, M.; Coustel, R.; Rouessac, V.; Roualdès, S.; Julbe, A. Microwave PECVD silicon carbonitride thin films: A FTIR and ellipsoporosimetry study. *Plasma Process. Polym.* **2016**, *13*, 258–265. [CrossRef]
31. Zhou, Y.; Josey, B.; Anim-Danso, E.; Maranville, B.; Karapetrova, J.; Jiang, Z.; Zhou, Q.; Dhinojwala, A.; Foster, M.D. In Situ Nanoscale Characterization of Water Penetration through Plasma Polymerized Coatings. *Langmuir* **2018**, *34*, 9634–9644. [CrossRef]
32. Blanchard, N.E.; Naik, V.V.; Geue, T.; Kahle, O.; Hegemann, D.; Heuberger, M. Response of Plasma-Polymerized Hexamethyldisiloxane Films to Aqueous Environments. *Langmuir* **2015**, *31*, 12944–12953. [CrossRef] [PubMed]
33. Rouessac, V.; Van Der Lee, A.; Bosc, F.; Durand, J.; Ayral, A. Three characterization techniques coupled with adsorption for studying the nanoporosity of supported films and membranes. *Microporous Mesoporous Mater.* **2008**, *111*, 417–428. [CrossRef]
34. Han, L.M.; Pan, J.-S.; Chen, S.-M.; Balasubramanian, N.; Shi, J.; Wong, L.S.; Foo, P.D. Characterization of carbon-doped SiO$_2$ low k thin films: Preparation by plasma-enhanced chemical vapor deposition from tetramethylsilane. *J. Electrochem. Soc.* **2001**, *148*, F148. [CrossRef]
35. Gallis, S.; Nikas, V.; Huang, M.; Eisenbraun, E.; Kaloyeros, A.E. Comparative study of the effects of thermal treatment on the optical properties of hydrogenated amorphous silicon-oxycarbide. *J. Appl. Phys.* **2007**, *102*, 24302. [CrossRef]
36. Yang, C.S.; Oh, K.S.; Choi, C.K.; Lee, H.J.; Lee, K.M. A study on the dielectric components of SiOC (-H) composite films deposited by using BTMSM/O 2-ICPCVD. *J. Korean Phys. Soc.* **2004**, *44*, 1102–1107.

37. Shamiryan, D.; Weidner, K.; Gray, W.D.; Baklanov, M.R.; Vanhaelemeersch, S.; Maex, K. Comparative study of PECVD SiOCH low-k films obtained at different deposition conditions. *Microelectron. Eng.* **2002**, *64*, 361–366. [CrossRef]
38. Yang, Z.; Li, Q.; Hua, R.; Gray, M.R.; Chou, K.C. Competitive adsorption of toluene and n-alkanes at binary solution/silica interfaces. *J. Phys. Chem. C* **2009**, *113*, 20355–20359. [CrossRef]